CETRA2024 15-17 May 2024, Cavtat, Croatia
8th International Conferenceon Road and Rail Infrastructure

USE OF DIGITAL IMAGING TO EVALUATE THE EFFECTIVENESS OF EPS GEOFOAM INCLUSIONS IN ALLEVIATING INTEGRAL BRIDGE APPROACH SETTLEMENTS

Dunja Perić, Justin Yenne
Department of Civil Engineering, Kansas State University, USA

Abstract

Absence of deck expansion joints in integral abutment bridges (IABs) offers multiple benefits that encompass increased redundancy, enhanced resilience, and diminished construction and lifetime maintenance costs. IAB's deck and girders undergo cyclic seasonal expansions and contractions accompanied with abutment translation and rotation that results in a near surface granular backfill collapse and creation of a void behind the abutment. The resulting loss of soil support leads to approach slab distress and severe approach slab settlement that often occurs shortly after the completion of construction. This research evaluates the effectiveness of a compressible wedge shaped inclusion, placed directly behind the IAB abutment, in alleviating the bridge approach settlement. This is accomplished by testing a downscaled physical model of the actual integral bridge abutment, piles and backfill. The abutment is subjected to 100 cycles of forward-backward displacement simulating cyclic seasonal superstructure expansion and contraction that occurs during 100 years of a bridge life cycle due to ambient temperature changes. Digital imaging correlation (DIC), a technique described as a non-contact optical deformation measurement, was used to capture the evolution of backfill displacements and strains. These mechanisms elucidate development of backfill failure and collapse mechanisms that are ultimately responsible for bridge approach settlement in IABs. Based on the results of DIC analysis and other measurements it was found that compressible inclusions favorably modify deformation mechanism in the backfill soil behind the expanded polystyrene (EPS) geofoam inclusion resulting in two times smaller settlement than in the case without and inclusions or reinforcements.

Keywords: bridge approach settlement, integral abutment bridge, near surface soil collapse

1 Introduction

Although absence of expansion joints and bearings in IABs results in multiple benefits including increased resilience, lowered construction and maintenance costs, smoother vehicular ride quality and more pleasing aesthetics, IABs also display more pronounced bridge approach settlements. Abutments of fully integral bridges are monolithically connected to piles, resulting in a continuous structural system where superstructure and substructure move together. Nevertheless, the absence of expansion joints results in cyclic seasonal expansion and contraction of deck and girders and corresponding translation and rotation or abutments that is accompanied with a near surface collapse of granular backfill behind the abutments. The collapse results in formation of a void behind the abutment and directly below the approach slab, leading to distress of approach slab due to the loss of soil support, and ultimately causing bridge approach settlement.

DOI: https://doi.org/10.5592/CO/CETRA.2024.1669

The problem gets exacerbated with each additional thermal cycle, thus requiring maintenance that often starts shortly after the bridge construction has been completed.
The main goal of this study was to assess effectiveness of a compressible wedge inclusions, placed behind the abutment, in alleviating the bridge approach settlement. This was accomplished by constructing the downscaled instrumented physical model of bridge abutment, piles and granular backfill. Seasonal cyclic translation and rotation of the abutment was modeled by moving the abutment top forward and backward throughout a 100 cycles total, thus representing the 100 years of a bridge life cycle [1]. A high-resolution camera and digital image correlation (DIC) software VIC-2D were used to capture the intricacies of deformation and failure mechanism of the granular backfill behind the compressible inclusion. Additionally, time history of lateral force and displacement was measured.

2 Experimental setup

A cuboid testing enclosure having a length of 1.5 m, width of 1.09 m and height of 1.12 m was constructed. Two smaller vertical walls and floor were made of two pieces of plywood, each 1.27 cm thick while the other two vertical walls were made of plexiglass, each 2.54 cm thick. Horizontal frames made of steel angles were placed around the container's top, bottom and at about depth of two thirds of the height, measured from the top. The container was placed directly on the floor and steel reaction frame was placed around it. A manually operated screw jack and load cell assembly were attached to the abutment top, enabling force measurement. Additionally, two linear variable differential transducers (LVDTs) measured horizontal displacement at the abutment top and vertical displacement of the backfill. The latter was used for validation of displacements obtained from digital imaging correlation software VIC-2D.
A 1:5 model of the stub abutment and two piles of "Bemis Road Bridge: F-4-20" over Nashua River in Fitchburg, Massachusetts [2] was constructed. Height and width of the abutment, made from solid aluminium, were equal to 0.5 m and 0.154 m respectively, while its length in the direction perpendicular to the plexiglass wall was 1.09 m. Two open ended steel pipe piles having outer diameter of 3.81 cm, wall thickness of 0.51 cm and length of 50.8 cm were screwed into the abutment bottom. The center to center spacing between the piles was 0.54 m. A photograph of the model with the compressible wedge inclusion after experiencing 100 loading cycles is shown in Figure 1. The wedge was constructed from three connected pieces of expanded polystyrene (EPS) geofoam, each having a height of 0.16 m. The widths of the top, middle and bottom pieces were 0.53 m, 0.36 m and 0.18 m respectively. All pieces were 1.09 m long in the direction perpendicular to the plexiglass wall. Compressive strength of EPS geofoam determined in accordance with ASTM D1621 [3] was 35 kPa at 10% deformation. Kansas river sand, which is classified as poorly graded sand (SP) according to the unified soil classification system (USCS), was used in the experiments. Coefficients of uniformity (C_u) and curvature (C_c) of Kansas river sand are 3.18 and 0.9 respectively [4]. Additionally, the minimum and maximum dry unit weights of Kansas sand are 16.02 and 18.85 kN/m^3 respectively, and its effective friction angle is 42° [4]. The air-dried Kansas river sand was thoroughly mixed, placed into the container and compacted to a relative density of 75%. The sand was compacted in five lifts below the bottom of abutment, each 10.16 cm thick, and remaining five lifts above the abutment bottom, each 9.65 cm thick.
Black sand was added within a distance of 2.54 cm of the plexiglass wall, above the bottom of the abutment to provide better contrast for digital imaging correlation (Figure 1).

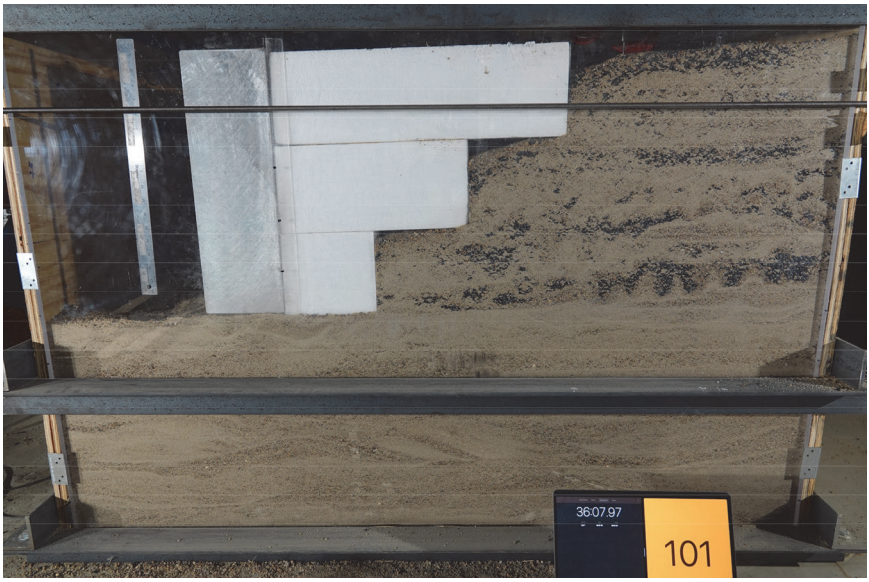

Figure 1 Testing enclosure showing abutment, EPS geofoam and Kansas river sand at the end of 100th cycle

2.1 Control mode

Each experiment started from neutral, nearly vertical position of the abutment corresponding to the end of sand compaction. The experiments were conducted in displacement control mode with intended displacement history and captured data depicted in Figure 1. Planned duration of each cycle was 30 seconds. Direction of positive displacement is away from the backfill and vice versa, negative displacement is directed into the backfill. Each load cycle started by imposing +3 mm displacement to the abutment top, followed by -3 mm, followed by another -3 mm and was completed with additional +3 mm.

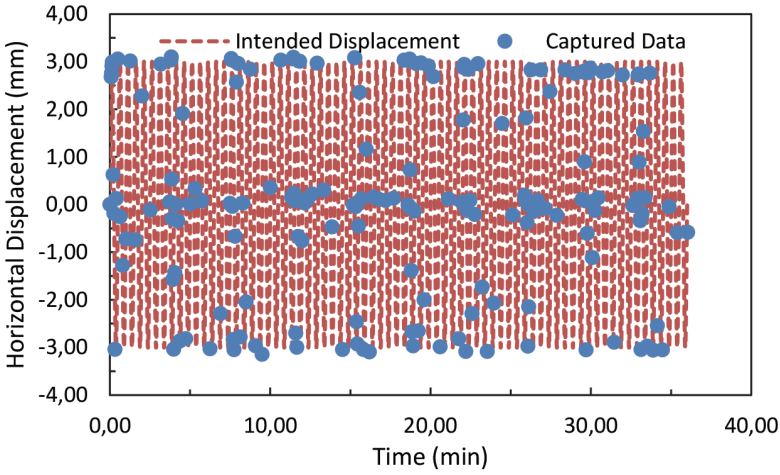

Figure 2 Intended history of horizontal displacement at the abutment top and captured data, experiment with wedge EPS geofoam

2.2 Camera and digital image correlation

Pictures were taken with Sony Cyber-Shot 20.9 megapixels DSC-RX10IV camera with effective picture size of 20.1 megapixels, allowing for a 5472 megapixels x 3648 megapixels pictures. The camera was placed 1.27 m away from the container, capturing the entire soil enclosure as shown in Figure 1. Pictures were taken per each 3 mm of displacement resulting in a total of four photos per each cycle.
A VIC-2D, commercial digital imaging correlation software, which can be customized and adapted to a particular experiment, was used in this study. The area of interest feature enabled the program to create a search patch comprising a group of pixels, L x L pixels in size, while cropping feature allowed for an area of interest of a size of 3800 pixels by 1400 pixels to be analysed.

3 Results

3.1 Force-displacement relationship and settlement

Figure 1 shows testing configuration at the end of the 100th cycle. The corresponding force displacement response is shown in Figure 3. Data points that belong to load cycles, for which data were recorded approximately every 7.5 seconds, are connected with straight lines while remaining data points are not connected. The data collection pattern can also be observed in Figure 2.
Figure 3 clearly shows that minimum force, which corresponds to the displacement of 3 mm stays approximately constant throughout the 100 cycles. On the contrary, the maximum force, which corresponds to a displacement of -3 mm increases with the increasing number of cycles. This is most likely closely connected to the collapse of sand at the interface of EPS geofoam and sand.

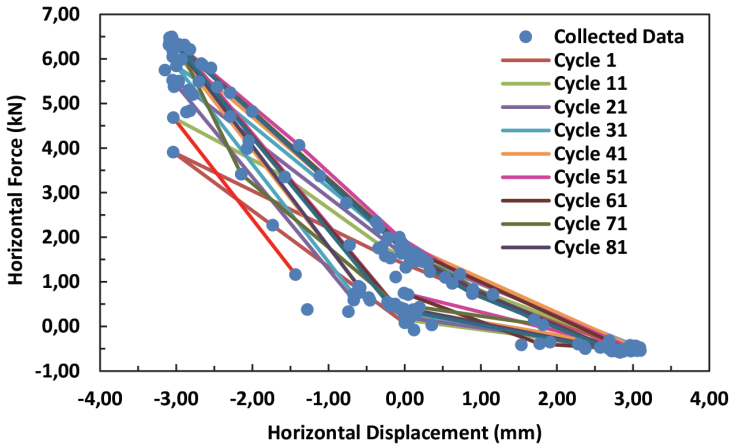

Figure 3 Horizontal force vs. horizontal displacement at the abutment top, experiment with wedge EPS geofoam

Figure 4 shows settlement at the contact of the backfill soil and the top EPS geofoam piece, as it compares to the settlement of the backfill at its contact with the abutment in the reference test without any inclusions. Therefore, the presence of the EPS geofoam wedge inclusion reduced the ultimate settlement of 8 cm in the reference configuration to 4 cm.

Additionally, the rate of settlement in the experiment with the EPS geofoam wedge inclusion is approximately constant and smaller than the rates of settlement observed in the reference experiment where the settlement rate in the latter gradually decreases. Finally, the settlement at the surface of the backfill occurs next to the abutment, where approach slab would be connected to the abutment, while the presence of geofoam inclusion displaces the location of the backfill settlement further away from the back face of the abutment.

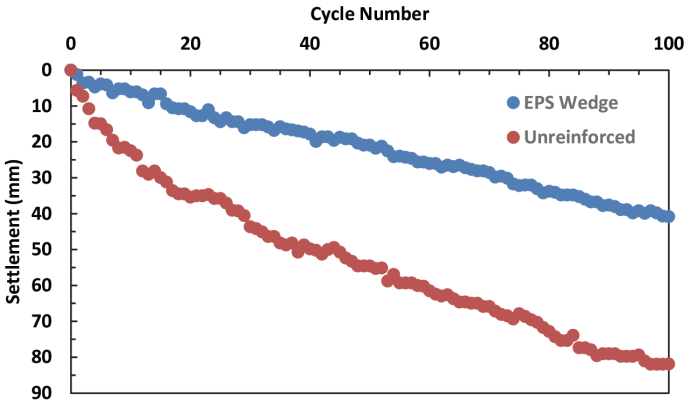

Figure 4 Settlement at the contact of backfill and top EPS geofoam piece, and at the contact of backfill and abutment in the reference test

3.2 Digital imaging correlation

VIC-2D uses patch brightness to identify the location of each patch in subsequent photographs, thus enabling calculation of displacement of each patch between any two photographs. Strain is then calculated based on the displacement. Lagrangian total shear strain (e_{xy}) between initial undeformed configuration and beginning of the first cycle is shown in Figure 5. The deformed configuration used to calculate the strain depicted in Figure 5 corresponds to the very first displacement of +3 mm, where abutment moves away from the backfill.

The miniature displacement vectors, which are superimposed to the heat map of Lagrangian shear strain shown in Figure 5, show that the sand within the active failure wedge moves to the left and downwards, as expected. Indeed, a series of shear bands that correspond to active failure are clearly visible. The shear band located next to the top EPS geofoam piece has propagated the furthest away from the lower right corner of the top EPS geofoam piece while the shear band next to the middle EPS geofoam piece has propagated to a smaller distance. It appears from Figure 5 that the very bottom shear band is at the inception stage. Maximum Lagrangian shear strains within these shear bands are approximately equal to 1.3%.

Simultaneously with the shear bands that signify active failure, primarily horizontally oriented shear bands develop at the contact of the sand and EPS geofoam inclusions. Maximum shear strains in these horizontal shear bands are approximately equal to -1%. These shear bands closely correspond the location of sand collapse induced by the temporary lack of confinement during the outward movement of the abutment. Therefore, the series of horizontally oriented shear bands is closely related to the backfill settlement and creation of the void that is ultimately responsible for bridge approach settlement.

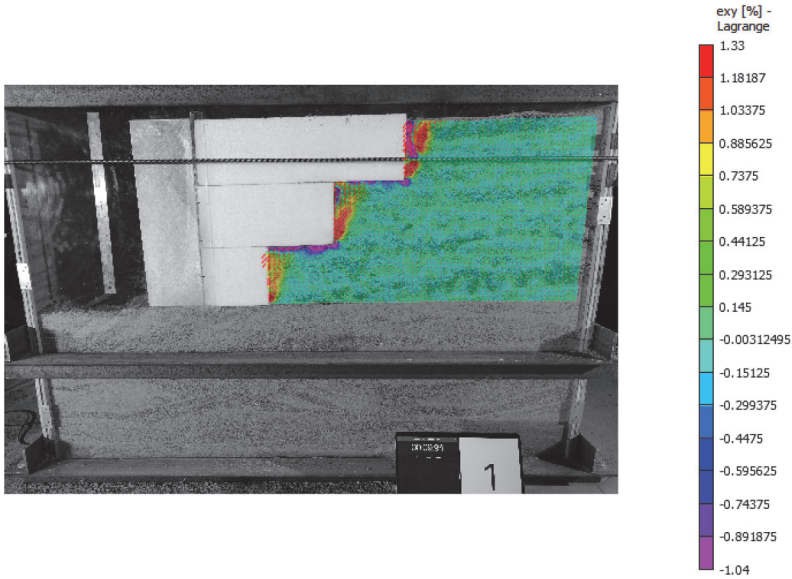

Figure 5 Heat map of total Lagrangian shear strain (e_{xy}) at the beginning of the first cycle corresponding of the abutment displacement of 3 mm away from the backfill

4 Conclusions

Experiments were conducted on a downscaled model of abutment and piles, which belong to the actual integral bridge, to evaluate the effectiveness of EPS geofoam wedge inclusion in alleviating bridge approach settlement. Poorly graded Kansas river sand was used as a backfill. A total of 100 cycles of forward-backward displacement having amplitude 3 mm were applied to the abutment top to simulate 100 years of seasonal superstructure expansions and contractions induced by ambient temperature changes. Use of high-resolution digital camera in conjunction with DIC provided non-contact optical deformation measurements.

It was found that presence of EPS geofoam wedge inclusion resulted in development of active failure demonstrated by a series of shear bands located in the soil behind each EPS geofoam piece. This series of inclined shear bands were accompanied by a different family of shear bands developing at the horizontal interface of the backfill soil and EPS geofoam inclusions. Therefore, the shape of EPS geofoam inclusion resulted in distributing one large shear band that was present in the test without any inclusions into a series of smaller shear bands. Additionally, the backfill collapse, which took place at near surface, in the experiment without inclusions was now distributed over three different levels.

Ultimately, the presence of compressible EPS geofoam inclusions halved the backfill settlement observed in the experiment without inclusions after 100 load cycles. While the backfill settlement in the experiment without inclusions occurred immediately behind the abutment, the presence of EPS geofoam moved the location of the maximum settlement further away from the abutment back face.

Acknowledgments

Both authors gratefully acknowledge funding provided by Kansas Department of Transportation through the KTRAN program.

References

[1] Maier, P., Kuhlman, U., Pfaffinger, M., Mensinger, M., Schneider, S., Zinke, T., Ummenhofer, T., Friedrich, H.: Sustainability Assessment of Bridges – Recent German Research Results, 10th Japanese-German Symposium, pp. 7-8, Munich, Germany, 16-19 September 2014.

[2] Perić, D., Miletić, M., Shah, B.R., Esmaeily, A., Wang, H.: Thermally induced soil structure interaction in the existing integral bridge, Engineering Structures, 106 (2016), pp. 484-494

[3] ASTM Standard D1621-16: Standard Test Method for Compressive Properties of Rigid Cellular Plastics, ASTM International, West Conshohocken, PA, 2023, DOI: 10.1520/D1621-16, www.astm.org

[4] Liu, H., Han, J. Parsons, R.L.: Settlement and Horizontal Earth Pressure behind Model Integral Bridge Abutment Induced by Seasonal Temperature Change, Journal of Getechincal and Geoenvironmental Engineering, 148 (2022) 6, DOI: 10.1061/%28ASCE%29GT.1943-5606.0002812